Biomedical Optics EXPRESS

Diverse effects of a 445 nm diode laser on isometric contraction of the rat aorta

Sang Woong Park,[1] Kyung Chul Shin,[1] Hyun Ji Park,[1] In Wha Lee,[2] Hyung-Sik Kim,[2] Soon-Cheol Chung,[2] Ji-Sun Kim,[2] Jae-Hoon Jun,[2] Bokyung Kim,[1] and Young Min Bae[1,*]

[1]*Department of Physiology, KU Open Innovation Center, Research Institute of Medical Science, Konkuk University School of Medicine, Chungju, Chungbuk 380-701, South Korea*

[2]*Department of Biomedical Engineering, BK21 + Research Institute of Biomedical Engineering, College of Biomedical and Health Science, Konkuk University, Chungju, Chungbuk 380-701, South Korea*

**ymbae30@kku.ac.kr*

Abstract: The usefulness of visible lasers in treating vascular diseases is controversial. It is probable that multiple effects of visible lasers on blood vessels and their unclear mechanisms have hampered the usefulness of this therapy. Therefore, elucidating the precise actions and mechanisms of the effects of lasers on blood vessels would provide insight into potential biomedical applications. Here, using organ chamber isometric contraction measurements, western blotting, patch-clamp, and *en face* immunohistochemistry, we showed that a 445 nm diode laser contracted rat aortic rings, both by activating endothelial nitric oxide synthase and by increasing oxidative stress. In addition to the effects on the endothelium, the laser also directly relaxed and contracted vascular smooth muscle by inhibiting L-type Ca^{2+} channels and by activating protein tyrosine kinases, respectively. Thus, we conclude that exposure to 445 nm laser might contract and dilate blood vessels in the endothelium and smooth muscle via distinct mechanisms.

OCIS codes: (170.0170) Medical optics and biotechnology; (170.5380) Physiology; (140.3450) Laser-induced chemistry; (140.7300) Visible lasers.

References and links

1. M. Correia, V. Thiagarajan, I. Coutinho, G. P. Gajula, S. B. Petersen, and M. T. Neves-Petersen, "Modulating the structure of EGFR with UV light: new possibilities in cancer therapy," PLoS One **9**(11), e111617 (2014).
2. T. Patino, U. Mahajan, R. Palankar, N. Medvedev, J. Walowski, M. Münzenberg, J. Mayerle, and M. Delcea, "Multifunctional gold nanorods for selective plasmonic photothermal therapy in pancreatic cancer cells using ultra-short pulse near-infrared laser irradiation," Nanoscale **7**(12), 5328–5337 (2015).
3. G. Alivizatos and A. Skolarikos, "Greenlight laser in benign prostatic hyperplasia: turning green into gold," Curr. Opin. Urol. **18**(1), 46–49 (2008).
4. K. Skriapas, W. Hellwig, M. Samarinas, U. Witzsch, and E. Becht, "Green light laser (KTP, 80 W) for the treatment of benign prostatic hyperplasia," Minerva Urol. Nefrol. **62**(2), 151–156 (2010).
5. M. H. Gold, W. Sensing, and J. A. Biron, "Clinical efficacy of home-use blue-light therapy for mild-to moderate acne," J. Cosmet. Laser Ther. **13**(6), 308–314 (2011).
6. N. Matsumoto, K. Yoshikawa, M. Shimada, N. Kurita, H. Sato, T. Iwata, J. Higashijima, M. Chikakiyo, M. Nishi, H. Kashihara, C. Takasu, S. Eto, A. Takahashi, M. Akutagawa, and T. Emoto, "Effect of light irradiation by light emitting diode on colon cancer cells," Anticancer Res. **34**(9), 4709–4716 (2014).
7. R. Macfarlane, A. Teramura, C. J. Owen, S. Chase, R. de la Torre, K. W. Gregory, J. W. Peterson, R. Birngruber, J. A. Parrish, and N. T. Zervas, "Treatment of vasospasm with a 480-nm pulsed-dye laser," J. Neurosurg. **75**(4), 613–622 (1991).
8. M. K. Y. Morimoto, H. Matsuo, and T. Arai, "Low-intensity Light Induces Vasomotion," Med. Biol. Eng. Comput. **34**, 283–284 (1996).
9. X. Gao and D. Xing, "Molecular mechanisms of cell proliferation induced by low power laser irradiation," J. Biomed. Sci. **16**(1), 4 (2009).
10. G. A. Knock and J. P. Ward, "Redox regulation of protein kinases as a modulator of vascular function," Antioxid. Redox Signal. **15**(6), 1531–1547 (2011).
11. R. Lu, A. Alioua, Y. Kumar, P. Kundu, M. Eghbali, N. V. Weisstaub, J. A. Gingrich, E. Stefani, and L. Toro, "c-Src tyrosine kinase, a critical component for 5-HT2A receptor-mediated contraction in rat aorta," J. Physiol. **586**(16), 3855–3869 (2008).
12. D. J. Sung, H. J. Noh, J. G. Kim, S. W. Park, B. Kim, H. Cho, and Y. M. Bae, "Serotonin contracts the rat

#242957 Received 18 Jun 2015; revised 12 Aug 2015; accepted 14 Aug 2015; published 21 Aug 2015

mesenteric artery by inhibiting 4-aminopyridine-sensitive Kv channels via the 5-HT2A receptor and Src tyrosine kinase," Exp. Mol. Med. **45**(12), e67 (2013).
13. H. S. Leung, X. Yao, F. P. Leung, W. H. Ko, Z. Y. Chen, M. Gollasch, and Y. Huang, "Cilnidipine, a slow-acting Ca2+ channel blocker, induces relaxation in porcine coronary artery: role of endothelial nitric oxide and [Ca2+]i," Br. J. Pharmacol. **147**(1), 55–63 (2006).
14. Y. M. Bae, A. Kim, J. Kim, S. W. Park, T. K. Kim, Y. R. Lee, B. Kim, and S. I. Cho, "Serotonin depolarizes the membrane potential in rat mesenteric artery myocytes by decreasing voltage-gated K+ currents," Biochem. Biophys. Res. Commun. **347**(2), 468–476 (2006).
15. L. J. Ignarro, "Nitric oxide as a unique signaling molecule in the vascular system: a historical overview," J. Physiol. Pharmacol. **53**(4 Pt 1), 503–514 (2002).
16. D. B. Kim-Shapiro, A. N. Schechter, and M. T. Gladwin, "Unraveling the reactions of nitric oxide, nitrite, and hemoglobin in physiology and therapeutics," Arterioscler. Thromb. Vasc. Biol. **26**(4), 697–705 (2006).
17. S. Dimmeler and A. M. Zeiher, "Nitric oxide-an endothelial cell survival factor," Cell Death Differ. **6**(10), 964–968 (1999).
18. M. Ziche, L. Morbidelli, E. Masini, S. Amerini, H. J. Granger, C. A. Maggi, P. Geppetti, and F. Ledda, "Nitric oxide mediates angiogenesis in vivo and endothelial cell growth and migration in vitro promoted by substance P," J. Clin. Invest. **94**(5), 2036–2044 (1994).
19. C. H. Chen, H. S. Hung, and S. H. Hsu, "Low-energy laser irradiation increases endothelial cell proliferation, migration, and eNOS gene expression possibly via PI3K signal pathway," Lasers Surg. Med. **40**(1), 46–54 (2008).
20. J. Zhang, D. Xing, and X. Gao, "Low-power laser irradiation activates Src tyrosine kinase through reactive oxygen species-mediated signaling pathway," J. Cell. Physiol. **217**(2), 518–528 (2008).
21. J. Li, W. Li, B. T. Altura, and B. M. Altura, "Peroxynitrite-induced relaxation in isolated canine cerebral arteries and mechanisms of action," Toxicol. Appl. Pharmacol. **196**(1), 176–182 (2004).
22. A. K. Brzezinska, D. Gebremedhin, W. M. Chilian, B. Kalyanaraman, and S. J. Elliott, "Peroxynitrite reversibly inhibits Ca(2+)-activated K(+) channels in rat cerebral artery smooth muscle cells," Am. J. Physiol. Heart Circ. Physiol. **278**(6), H1883–H1890 (2000).
23. F. M. Faraci, "Reactive oxygen species: influence on cerebral vascular tone," J. Appl. Physiol. **100**(2), 739–743 (2006).
24. Y. Fukuzaki, H. Sugawara, B. Yamanoha, and S. Kogure, "532 nm low-power laser irradiation recovers γ-secretase inhibitor-mediated cell growth suppression and promotes cell proliferation via Akt signaling," PLoS One **8**(8), e70737 (2013).
25. G. Shefer, U. Oron, A. Irintchev, A. Wernig, and O. Halevy, "Skeletal muscle cell activation by low-energy laser irradiation: a role for the MAPK/ERK pathway," J. Cell. Physiol. **187**(1), 73–80 (2001).
26. Q. Gu, L. Wang, F. Huang, and W. Schwarz, "Stimulation of TRPV1 by Green Laser Light," Evid. Based Complement. Alternat. Med. **2012**, 857123 (2012).
27. L. Wang, D. Zhang, and W. Schwarz, "TRPV Channels in Mast Cells as a Target for Low-Level-Laser Therapy," Cells **3**(3), 662–673 (2014).
28. W. Z. Yang, J. Y. Chen, J. T. Yu, and L. W. Zhou, "Effects of low power laser irradiation on intracellular calcium and histamine release in RBL-2H3 mast cells," Photochem. Photobiol. **83**(4), 979–984 (2007).

1. Introduction

Laser therapy has been used for treating cancer, diabetic retinopathy, as well as skin and vascular diseases. Recently, ultraviolet (UV) lasers have been suggested to be useful for cancer therapy owing to their ability to modulate the structure of EGFR [1]. However, UV lasers also affect normal cells. Infrared lasers can be used for cancer therapy [2], but they can induce cell or tissue damage through high temperatures. Green lasers (520–570 nm) are used for the treatment of benign prostatic hyperplasia [3, 4]. Blue lasers (360–480 nm) are used for skin (acne) and cancer therapy [5, 6]. In addition, a previous study demonstrated that a 480 nm laser could be used for treating vasospasms [7]. However, the effects of visible laser on blood vessels are controversial. Morimoto et al. [8] reported that a 381 nm laser induced nitric oxide (NO) synthesis and relaxed blood vessels. In contrast, an 800 nm laser induced vasoconstriction by elevating the temperature. In addition, a blue laser (458 nm) and green laser (514 nm) relaxed and contracted blood vessels, respectively [8]. Elucidating the precise actions and mechanisms of laser-based effects on blood vessels would provide insight into potential biomedical applications in the field of laser therapy.

Blood vessels regulate blood flow by altering their diameter, which is primarily regulated by the contractile status of the vascular smooth muscle (VSM) that comprises the medial layer of blood vessels. Blood vessels are composed of three layers: inner endothelial, medial smooth muscle, and outer adventitia. In addition to the medial VSM, the inner endothelial cells also play critical roles in regulating blood vessel diameter. For example, endothelial cells release NO in response to various stimuli such as acetylcholine and shear force. NO is

#242957 Received 18 Jun 2015; revised 12 Aug 2015; accepted 14 Aug 2015; published 21 Aug 2015

synthesized by endothelial NO-synthase (eNOS) and is well known as an endothelium-derived relaxing or hyperpolarizing factor (EDRF or EDHF). NO improves blood flow by relaxing VSM and dilating vessels. However, under certain circumstances, including oxidative stress, NO is rapidly converted to a reactive and unstable form such as peroxynitrite ($ONOO^-$), which regulates blood vessels differently than NO. In addition to relaxing blood vessels through NO, endothelial cells can also contract vessels via endothelial contracting factors such as endothelin-1. Therefore, examining the separate effects of laser exposure on endothelial cells and VSMs would be very helpful for understanding the consequences of laser exposure on blood vessels.

In this study, using electrophysiology, immunohistochemistry, and an isometric organ chamber mechanical approach, we endeavored to elucidate the mechanistic basis of the diverse effects of laser exposure on the rat aorta. Our results clearly indicate that the 445 nm diode laser paradoxically contracted the isometric aortic rings by activating eNOS in endothelial cells. In VSM, the 445 nm laser either contracted or relaxed the aortic rings by increasing tyrosine phosphorylation or by inhibiting L-type Ca^{2+} channels (VLCC), respectively. Therefore, we conclude that the 445 nm laser contracts or dilates blood vessels through distinct mechanisms in the endothelium and VSM.

2. Materials and methods

2.1 Tissue and cell preparation

Male Sprague–Dawley (SD) rats (age: 11 weeks) were used for the experiments. All experiments were conducted in accordance with the National Institutes of Health guidelines for the care and use of animals, and the Institutional Animal Care and Use Committee of Konkuk University approved this study. Rats were sacrificed by exposure to an increasing concentration of carbon dioxide or exsanguinated by severing the carotid arteries under deep ketamine-xylazine anesthesia. We used the aorta for organ chamber isometric contraction measurements and *en face* experiments. In addition, we used the rat aortic smooth muscle cell line A7r5 for western blot analysis and electrophysiological recordings. A7r5 cells were cultured in HyClone Dulbecco's Modified Eagle's Medium (DMEM) containing 10% fetal bovine serum (FBS) and 1% penicillin-streptomycin.

2.2 Solutions and drugs

Bicarbonate-buffered physiological salt solution (PSS) was used as the bath solution for the organ chamber mechanics experiments. PSS was composed of 136.9 mM NaCl, 5.4 mM KCl, 1.5 mM $CaCl_2$, 1.0 mM $MgCl_2$, 23.8 mM $NaHCO_3$, and 0.01 mM EDTA. The normal Tyrode (NT) solution was used as the bathing solution for patch-clamp experiments. NT solution contained 143 mM NaCl, 5.4 mM KCl, 0.33 mM NaH_2PO_4, 1.8 mM $CaCl_2$, 0.5 mM $MgCl_2$, 5 mM HEPES, and 11 mM glucose, adjusted to pH 7.4 with NaOH. The internal pipette solution contained 40 mM CsCl, 100 mM methane sulfonate-Cl, 5 mM MgATP, 10 mM HEPES, and 10 mM 1,2-bis(aminophenoxy)ethane-*N,N,N′,N′*-tetraacetic acid, adjusted to pH 7.2 with CsOH. All chemicals were purchased from Sigma.

2.3 Irradiation with a 445 nm laser

A Levin series blue laser (LaserTo, Hong Kong) was used at a wavelength of 445 nm. The laser source was equipped with a built-in simple lens system consisting of a beam expander and negative lens, to deliver a collimated beam to the sample. We customized the laser to be able to vary the output power, irradiation time, and synchronization with the patch clamp system. Tissues and cells were directly irradiated using a laser power of 300 mW and a 4 mm spot diameter at a distance of 20 cm. The output power and spot diameter were measured using a power meter 1918-R (Newport, USA) and a beam profiler SP620U (Ophir-Spiricon LLC, USA), respectively.

#242957 Received 18 Jun 2015; revised 12 Aug 2015; accepted 14 Aug 2015; published 21 Aug 2015

2.4 Organ chamber isometric contraction measurements

Arterial rings were mounted vertically on two L-shaped stainless steel wires in a 3-mL tissue chamber for tension measurements. One wire was attached to a micromanipulator and the other to an isometric force transducer (FT03, Grass, West Warwick, RI, USA). Changes in isometric force were digitally acquired at 1 Hz using a PowerLab data acquisition system (AD Instruments, Colorado Springs, CO, USA). Resting tension was set to 1 g using the micromanipulator. The lengths of aortic rings were ~3 mm, and the widths (the outer diameter) of the aortic rings were ~2 mm in the resting state. After the aortic rings were stretched with 1 g of tension, the ring was changed to an ellipsoid shape with a longer diameter of ~3 mm. After a 60 min equilibration under resting tension in a tissue chamber filled with PSS, the rings were sequentially exposed to 70 mM KCl-PSS (10 min) and PSS (15 min) three times for stabilization. High KCl (35 or 70 mM) PSS was prepared by replacing NaCl with equimolar KCl in PSS. Bath solutions were thermostatically controlled at 37°C and were continuously saturated with a mixture of 95% O_2 in 5% CO_2 to achieve pH 7.4.

2.5 Western blot analysis

The A7r5 cell line was used for western blot analysis. Cells were grown to 80% confluence and starved in DMEM without FBS for 12 h prior to experiments. After starvation, the cells were laser irradiated for 1, 3, and 5 min in the microtubes (Axygen, Union City, CA, USA) at 25°C. Cells were then washed twice with PBS and lysed using RIPA buffer (TNT Research, Seoul, South Korea). Samples were run on a 10% SDS-polyacrylamide non-reducing gel and then transferred to a polyvinylidene fluoride (PVDF) membrane (Millipore, Bedford, MA, USA). Rabbit primary antibodies against p-tyrosine (1:500, Millipore) and secondary antibodies conjugated with horseradish peroxidase (1:2,000, Cell Signaling Technology, Danvers, MA, USA) were used. Signals were visualized using a Las-4000 system (Fujifilm, Tokyo, Japan).

2.6 En face immunohistochemistry

Aortic tissues were cut in half on a silicone chamber. The endothelial layer was irradiated for 1, 3, and 5 min, using the laser. The aortic tissues were treated with 4% paraformaldehyde for 30 min, 0.1% Triton X-100 for 10 min, and 5% BSA blocking solution for 1 h. Then, the tissues were incubated overnight at 4°C with goat primary antibodies against pNOS3 (phosphorylated eNOS, 1:100, Santa Cruz) and rabbit primary antibodies against NOS3 (1:100, BD Tranduction Laboratories). For fluorescence imaging, Cy2-conjugated anti-rabbit secondary antibodies (1:1,000, Alomone Labs) and Alexa 594-conjugated anti-goat secondary antibodies were used (1:1,000, Life Technologies). We used TOPRO-3 (1:1,000, Life Technologies) for DNA staining. The aortic tissues were imaged using confocal microscopy (Zeiss LSM-710).

2.7 Electrophysiological recordings

We used a conventional whole-cell configuration for the patch-clamp technique to record membrane currents. Either an EPC8 (HEKA, Mahone Bay, Nova Scotia, Canada) patch clamp amplifier with a DAQPad-6070E interface (National Instrument, Austin, TX, USA) or an Axopatch 200B patch-clamp amplifier with a Digidata 1200 interface (Axon Instruments, Foster City, CA, USA) was used. Data was digitized using custom-built software (R-clamp, by Dr. Ryu SY) at a sampling rate of 10 kHz. The data were low-pass filtered at 1 kHz and saved for analysis. Voltage pulse generation was also controlled using the R-clamp software. Patch pipettes were pulled from borosilicate capillary tubes (Clark Electromedical Instruments, Pangbourne, UK) using a puller (PP-83, Narishige, Tokyo, Japan). We used patch pipettes with a resistance of 2–4 MΩ when filled with the above-mentioned pipette solution. All experiments were carried out at room temperature (20–25°C).

#242957 Received 18 Jun 2015; revised 12 Aug 2015; accepted 14 Aug 2015; published 21 Aug 2015

2.8 Data analysis

Origin 8.0 software (MicroCal Software Inc., Northampton, MA, USA) was used for data analysis. The results are shown as mean ± standard error. Paired or independent Student's *t*-tests were used to test for significance, and $p < 0.05$ was considered significant.

3. Results

3.1 Effects of 445 nm laser-irradiation on isometric tension in aortic rings: roles of endothelium and smooth muscle tyrosine phosphorylation

A schematic illustration showing the experimental setup for the isometric tension measurement and laser irradiation is shown in Fig. 1(E). In Figs. 1(A) and 1(B), the functional presence of the endothelium was examined by the presence or absence of acetylcholine-induced relaxation after contraction using 70 mM KCl. The irradiation was performed using a 445 nm laser (for 5 min) after the aortic rings were pre-contracted using 35 mM KCl bathing solution. The laser-induced contraction or relaxation was then normalized to the pre-contraction condition for quantitative comparison. Under these conditions, the 445 nm laser irradiation typically resulted in an initial transient and minimal relaxation followed by strong contraction in the intact endothelium aortic rings (Fig. 1(A)). In contrast, the 445 nm laser typically resulted in initial relaxation followed by relatively small contraction in endothelium-denuded aortic rings (Fig. 1(B)). In Fig. 1(B), we regarded the time-dependent decrease in initial relaxation as 'late contraction' on the basis of the result shown in Fig. 1(C) (see below). Tyrosine phosphorylation by protein tyrosine kinase (PTK) in vascular smooth muscles frequently mediated agonist-, oxidative stress-, and light irradiation-induced vasoregulation, which include vasocontraction [9–12]. In order to investigate the role of PTK in endothelium-denuded aortic rings, we examined the effects of a broad-spectrum PTK inhibitor, genistein. In endothelium-denuded aortic rings, genistein (10 μM) blocked the late contraction, unmasking the sustained vasorelaxation. The results in Figs. 1(B) and 1(C) indicate that in the absence of the endothelium, smooth muscle PTK mediated the late contraction induced by the 445 nm laser. In addition, the results in Figs. 1(A) and 1(B) suggest that the 445 nm laser induced initial relaxation and late contraction of aortic rings and that the endothelium was involved in the mechanism of late vasocontraction. The results in Figs. 1(A)–1(C) are summarized and compared in Fig. 1(D). In order to confirm that the 445 nm laser indeed activated PTK in aortic smooth muscle, we examined the effect of the laser on A7r5 smooth muscle cells. The experimental setup for laser irradiation of A7r5 cells is schematically illustrated in Fig. 1(F) as a figure inset. Western blotting experiments clearly showed time-dependent phosphorylation of tyrosine residues in protein homogenates of A7r5 cells (Fig. 1(F)) induced by 445 nm laser irradiation, which supports the hypothesis that activation of PTK by laser irradiation contracted the VSM in the absence of endothelium. The laser power measured between water depths of 3 mm and 15 mm was unchanged (Fig. 1(G)), indicating that nearly the same power of laser was applied in organ chamber isometric tension experiments, in microtube western blot experiments, and in *en face* immunohistochemistry experiments (Fig. 2(F)).

#242957 Received 18 Jun 2015; revised 12 Aug 2015; accepted 14 Aug 2015; published 21 Aug 2015

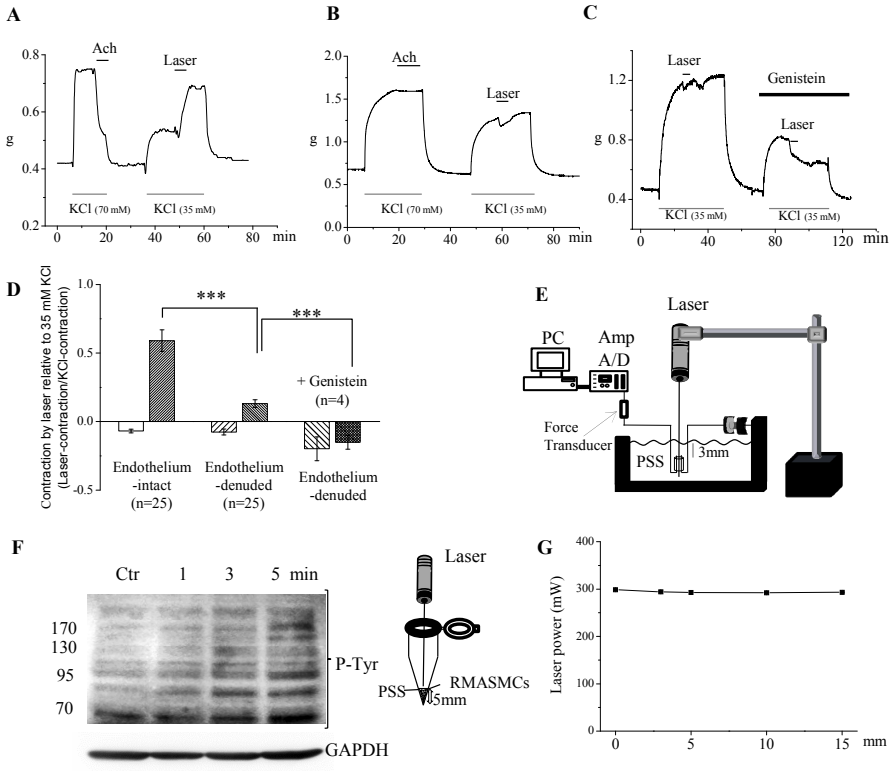

Fig. 1. **Effects of 445 nm diode laser irradiation on the isometric contractions of aortic rings.** A. Representative traces showing the effects of 445 nm laser-irradiation on the isometric contraction of an 'endothelium-intact' rat aortic ring. Intact function of the endothelium was verified by demonstrating acetylcholine (Ach, 100 μM)-induced relaxation after pre-contraction using 70 mM KCl. B. Representative traces showing the effects of 445 nm laser-irradiation on the isometric contraction of an 'endothelium-denuded' rat aortic ring. Removal of the endothelium was verified by demonstrating there was little effect of Ach after pre-contraction using 70 mM KCl. C. Representative traces showing the effects of a general protein tyrosine kinase (PTK) inhibitor, genistein (10 μM). In the presence of genistein, the 445 nm laser markedly relaxed the 'endothelium-denuded' aortic ring without subsequent contraction. D. Summary of the effects of 445 nm laser-irradiation on blood vessels with endothelium (left), without endothelium (middle), and without endothelium pretreated with genistein (right). Negative values indicate vasorelaxation and positive values vasoconstriction, respectively. E. Schematic illustration for isometric contraction experiments. F. Representative western blotting of whole-protein homogenate from A7r5 cells that were irradiated with the 445 nm laser as indicated. Similar results were obtained in three subsequent independent experiments. Schematic illustration showing the experimental setup for laser irradiation to A7r5 cells is shown as a figure inset. G. Effect of water level on the applied power of laser. The y-axis indicates laser power, measured as described in the methods section, and the x-axis indicates the depth of water (mm). The values are averages of 10 repeated measurements. ***indicates $p < 0.001$ between two groups. Numbers in parentheses indicate numbers of animals tested.

3.2 Activation and subsequent rapid oxidation of endothelial NO mediate 445 nm laser-induced vasocontraction

Since the 445 nm laser induced marked contraction in an endothelium-dependent manner, we tested the hypothesis that endothelial NO is involved in laser-induced vasocontraction. In the presence of the eNOS inhibitor L-NAME (100 μM), 445 nm laser-induced vasocontraction was inhibited (Fig. 2(A)). In some aortic rings for which the contractile response was relatively small under the control conditions, pretreatment with L-NAME relaxed the aortic rings more markedly (Fig. 2(B)). Furthermore, we examined whether activation of

#242957 Received 18 Jun 2015; revised 12 Aug 2015; accepted 14 Aug 2015; published 21 Aug 2015

endothelium-dependent contractile factors such as endothelin-1 (ET-1) was involved in laser-induced vasocontraction. Pretreating with sulfisoxazole (10 μM), an inhibitor of the ET-1 receptor, however, did not affect laser-induced vasocontraction (Fig. 2(C)).

The results described above suggest that the 445 nm laser induced contraction of aortic rings by activating eNOS. Since the hypothesis that the activation of eNOS mediates vasocontraction seems paradoxical, we suspected that concomitant activation of oxidative stress by the 445 nm laser rapidly converted NO into a vasocontractile molecule such as $ONOO^-$. In support of this hypothesis, pretreatment using the antioxidant GSH (10 mM) markedly reduced laser-induced vasocontraction (Fig. 2(D)). The contraction and relaxation of intact endothelium aortic rings under the various conditions are summarized in Fig. 2(E). These results indicate that the endothelium-dependent contraction induced by the 445 nm laser was mediated by eNOS activation. To further address this hypothesis, we examined whether the 445 nm laser activated eNOS by *en face* immunohistochemistry. Irradiation using the 445 nm laser clearly resulted in phosphorylation of eNOS in the endothelium (Fig. 2(F)).

To further confirm that NO, which is derived from the activation of eNOS, is involved in laser-induced vasocontraction, we examined the effects of the NO-donor sodium nitroprusside (SNP) on laser irradiation-induced vasocontraction. In the presence of SNP, the 445 nm laser induced an even larger vasocontraction, whereas SNP reduced vasocontraction induced by 35 mM KCl (Fig. 3(A)). The 445 nm laser-induced contractions in the absence and presence of SNP are summarized and compared in Fig. 3(B).

Taken together, the data in Figs. 2 and 3 suggest that activation of eNOS, subsequent production of NO and its rapid conversion into an oxidative form might be involved in 445 nm laser-induced vasocontraction.

#242957 Received 18 Jun 2015; revised 12 Aug 2015; accepted 14 Aug 2015; published 21 Aug 2015

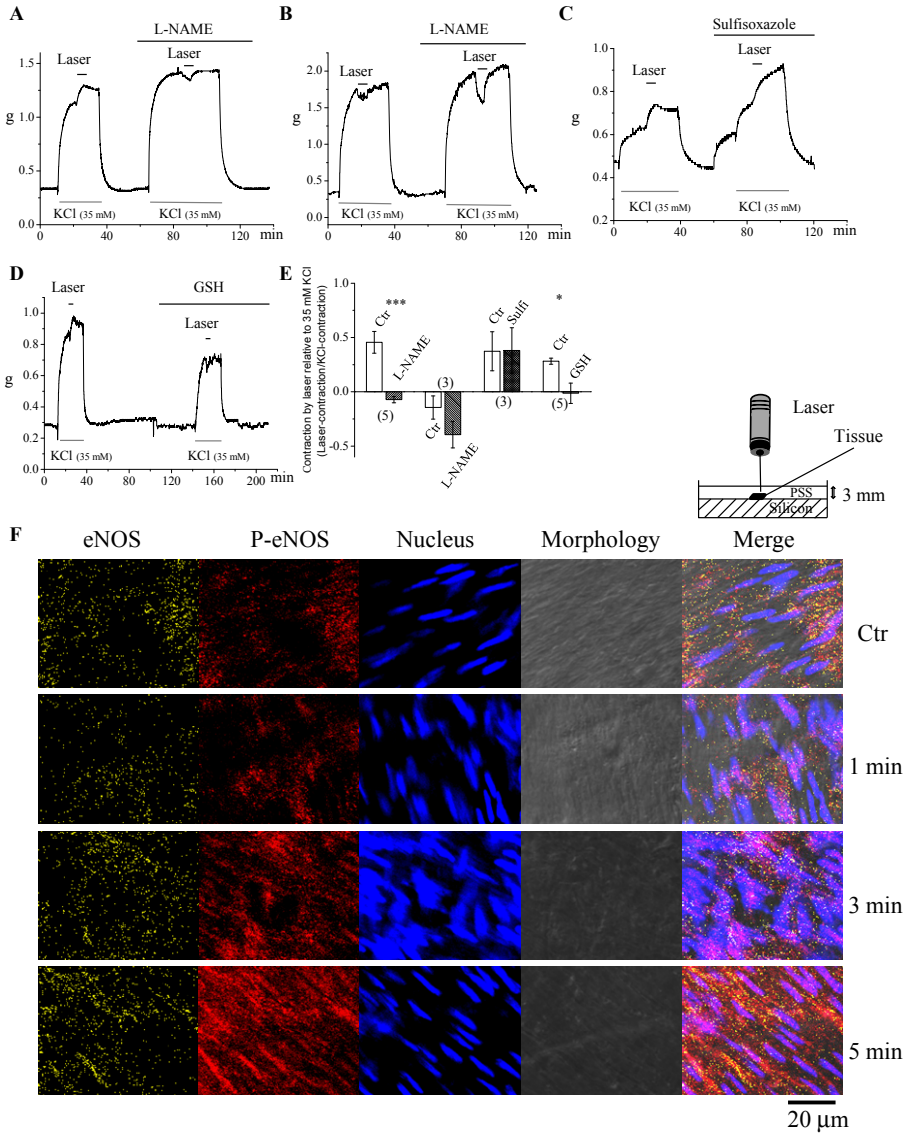

Fig. 2. **Effects of inhibitors of eNOS and endothelin-1 receptors, and reduced glutathione on 445 nm laser-induced effects in 'endothelium-intact' aortic rings.** A and B. To inhibit endothelial nitric oxide (NO) synthase (eNOS), L-N^G-Nitroarginine methyl ester (L-NAME, 100 μM) was used for pretreatment. Pretreating with L-NAME abolished 445 nm laser-induced vasocontraction, which is shown before treatment with L-NAME (A), or potentiated vasorelaxation when the control response was relaxation-dominant (B). C. Representative traces showing the effects of sulfisoxazole (inhibitor of ET-1 receptor, 10 μM). In the presence of sulfisoxazole, the 445 nm laser still markedly contracted 'endothelium-intact' aortic rings. D. Representative traces showing the effect of reduced glutathione (GSH, 10 mM). After GSH pretreatment, the 445 nm laser failed to contract the aortic ring. E. Summary of the results shown in Fig. 2(A)-2(D). Negative values indicate vasorelaxation and positive values vasoconstriction. F. *En face* immunohistochemistry of phosphorylated eNOS in aortic tissue. The experimental setup of laser irradiation for *en face* immunohistochemistry experiments is schematically illustrated as a figure inset. Yellow color indicates eNOS, red color indicates phosphorylated eNOS, and blue color indicates the nucleus. Laser irradiation increased phosphorylation of eNOS in a time-dependent manner (0, 1, 3, and 5 min). *indicates $p < 0.05$ vs. control (the first response before various pretreatments). ***indicates $p < 0.001$ vs. control. Numbers in parentheses indicate numbers of animals tested.

#242957 Received 18 Jun 2015; revised 12 Aug 2015; accepted 14 Aug 2015; published 21 Aug 2015

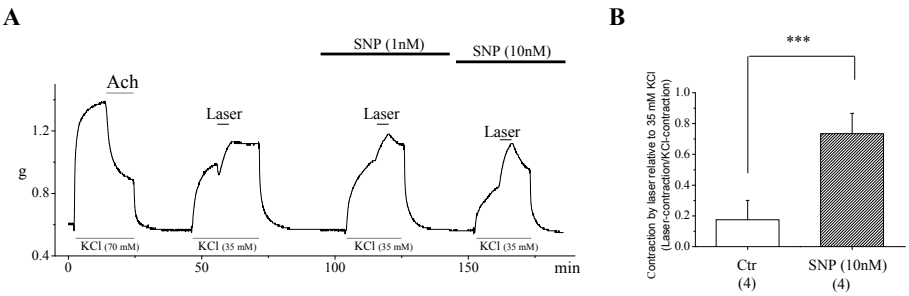

Fig. 3. **Effects of NO on 445 nm laser irradiation-induced vasocontraction in 'endothelium-intact' aortic rings.** A. Representative traces showing the effects of the NO-donor sodium nitroprusside (SNP). Intact function of the endothelium was verified by demonstrating acetylcholine (Ach, 100 μM)-induced relaxation at the beginning of the recording. SNP potentiated 445 nm laser-induced vasocontraction as well as abolished the initial minimal vasorelaxation in a concentration-dependent manner. SNP (10 nM) decreased the 35 mM KCl-induced vasocontraction, as was previously reported [13]. B. Summary of the effects of SNP (10 nM). ***indicates $p < 0.001$ vs. control (before SNP treatment). Numbers in parentheses indicate numbers of animals tested.

3.3 Effects of laser irradiation on VSM without endothelium

Next, we examined the mechanistic basis for how the 445 nm laser regulated the contraction of aortic rings without endothelium. Generally, depolarization and subsequent activation of voltage-gated VLCCs play an important role in the contraction of VSM. To assess the contribution of VLCC-dependent and -independent regulation of 445 nm laser-induced changes in the contraction of VSM, 5-HT (instead of 35 mM KCl) was used for pre-contraction in some experiments. The 5-HT-induced VSM contraction was reportedly Src tyrosine kinase-dependent [11] and was composed of ~70% VLCC-dependent and ~30% VLCC-independent contractions [12, 14]. Irradiation with the 445 nm laser initially relaxed endothelium-denuded aortic rings pre-contracted with 5-HT (10 μM), but was followed by contraction (Fig. 4(A)). These results were qualitatively similar to those in Fig. 1(B), where pre-contraction was induced using 35 mM KCl. To exclude the role of VLCC in vasocontraction, endothelium-denuded aortic rings were pre-contracted with 5-HT in the presence of nifedipine (10 μM, a VLCC blocker). Under these conditions, the 445 nm laser markedly contracted the aortic ring (Fig. 4(B)). The laser-induced initial vasorelaxation and subsequent contraction in the absence and presence of nifedipine in aortic rings are summarized and compared in Fig. 4(C). The results in Fig. 4(A) and 4(B) indicate that the 445 nm laser both relaxed and contracted the VSM in the absence of the endothelium and that the VLCC was involved in the mechanism of the laser-induced relaxation of VSM. Accordingly, laser irradiation inhibited VLCC currents in patch-clamp experiments (Fig. 4(D)). The results shown in Fig. 4 together with Figs. 1(B), 1(C), and 1(F) suggest that in the absence of the endothelium, the 445 nm laser relaxed and contracted the VSM by inhibiting VLCCs and activating PTK, respectively.

#242957 Received 18 Jun 2015; revised 12 Aug 2015; accepted 14 Aug 2015; published 21 Aug 2015

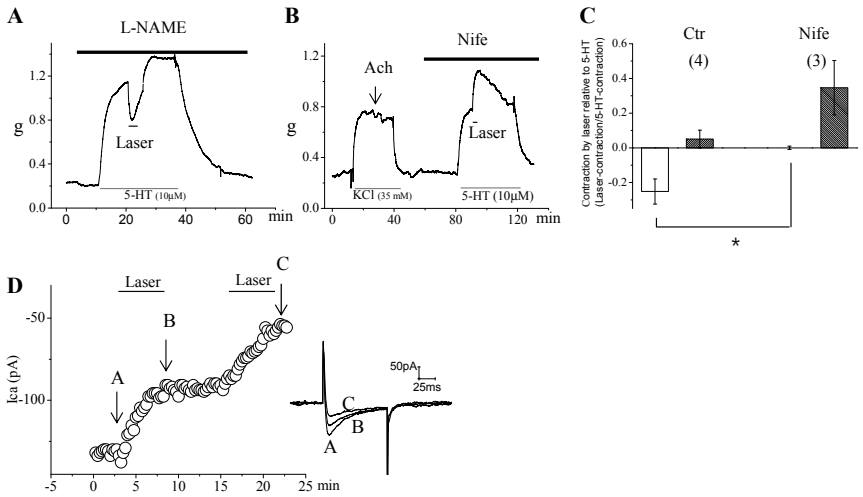

Fig. 4. **Effects of 445 nm laser irradiation on vascular smooth muscle (VSM) without endothelium.** A. Representative traces showing the effects of 445 nm laser irradiation after 5-HT pre-contraction in an 'endothelium-denuded' aortic ring. To ensure the exclusion of eNOS, L-NAME (100 μM) was used for pretreatment. Without the endothelium, laser irradiation relaxed and then contracted (or decrease of relaxation) the aortic ring. Note that the response is qualitatively similar to those in Fig. 1(B), where pre-contraction was induced by 35 mM KCl. B. Representative traces showing the effects of pretreating with nifedipine (10 μM), a VLCC blocker. In the presence of nifedipine, the 445 nm laser markedly contracted the 'endothelium-denuded' aortic ring without relaxation. The minimal effect of Ach (100 μM) indicated that most of the endothelium was successfully removed. C. Summary of the effects of nifedipine on 445 nm laser irradiation-induced responses of 'endothelium-denuded' aortic rings. D. Effects of 445 nm laser irradiation on VLCC currents. VLCC currents were elicited by repetitive depolarizing voltage steps to 0 mV from a holding potential of −70 mV. Representative time-plots of the peak VLCC current. The duration of laser irradiation is indicated as a solid bar. The raw current traces at the indicated points are shown as figure insets. Similar results were obtained in seven subsequent independent experiments. *indicates $p < 0.05$ vs. control. Numbers in parentheses indicate numbers of animals tested.

4. Discussion

In this study, we have demonstrated diverse effects of 445 nm blue laser irradiation on rat aorta and the A7r5 cell line. Irradiation with a relatively low-power 445 nm laser contracted the aortic ring by activating eNOS in the endothelium and by increasing oxidative stress. At the same time, the VSM itself was also affected by the 445 nm laser, where contraction was mediated by tyrosine phosphorylation and relaxation by VLCC inhibition.

4.1 Irradiation with a 445 nm laser contracted aortic rings by activating eNOS

It appears paradoxical that activation of eNOS resulted in the contraction of blood vessels. The results in Figs. 1 and 2 with L-NAME and *en face* immunohistochemistry of p-eNOS, however, support the hypothesis that activation of eNOS mediates 445 nm laser-induced vasocontraction. Furthermore, the results in Fig. 3 with SNP directly demonstrate that increasing NO potentiated 445 nm laser-induced vasocontraction. The endothelium-derived contractile factor ET-1 was not involved in 445 nm laser-induced vasocontraction, since a blocker of the ET-1 receptor did not inhibit laser-induced contraction (Fig. 2(C)).

NO has been well recognized as a potent vasodilator. NO is primarily synthesized by eNOS in the endothelium in response to various (patho-) physiological stimuli such as parasympathetic activation (acetylcholine) and shear force. In the clinical setting, NO relaxes blood vessels by activating cGMP and protein kinase G. The potent vasorelaxing actions of NO are well reviewed in the literature [15, 16]. In addition to vasorelaxation, NO also

#242957 Received 18 Jun 2015; revised 12 Aug 2015; accepted 14 Aug 2015; published 21 Aug 2015

regulates endothelial cell growth, migration, and apoptosis [17, 18]. Consistent with results of the present study, a previous report also indicated that low-energy laser irradiation increased eNOS activity through phosphorylation of PI3K/Akt in human umbilical vein endothelial cells (HUVECs) [19].

We hypothesized that activation of oxidative stress by the 445 nm laser might contribute to eNOS activation-dependent vasocontraction, and the results in Fig. 2(D) with GSH support this hypothesis. Consistent with this result, a previous study also reported that low-power laser irradiation activated Src tyrosine kinase through reactive oxygen species (ROS) in HeLa cells [20]. ROS can bind to NO produced by activated eNOS to produce reactive nitrogen species (RNS) such as $ONOO^-$. Although still controversial [21], RNS such as peroxynitrite have been reported to contract blood vessels [22, 23].

Taken together, we demonstrated that 445 nm laser irradiation activated both eNOS and oxidative stress in aortic rings to subsequently produce RNS/ROS, which induced the contraction of aortic rings.

4.2 Irradiation with the 445 nm laser activated PTKs of VSM

Without the endothelium, the 445 nm laser still contracted aortic rings after an initial relaxation (Figs. 1(B) and 4(A)). The 445 nm laser-induced vasocontraction became more evident when VLCCs were blocked using nifedipine (Fig. 4(B)). This result indicates both that 445 nm laser-induced vasorelaxation was mediated by modulation of VLCCs and that laser-induced vasocontraction was independent of VLCCs. We hypothesized that phosphorylation of certain VSM proteins that are related to the contraction of VSM might mediate VLCC-independent, laser-induced vasocontraction. In support of this, pretreating with genistein, which is a general inhibitor of PTKs, abolished the contractile response of endothelium-denuded aortic ring (Fig. 1(C)), unmasking a marked and sustained laser-induced relaxation. From these results, we suggested that 445 nm laser irradiation contracted the VSM without endothelium by inducing the phosphorylation of tyrosine residues of proteins that are associated with VSM contraction. We also observed the 445 nm laser-induced phosphorylation of numerous tyrosine residues as determined by western blot analysis (Fig. 1(F)). In fact, this observation agrees with the previous finding that low-power laser irradiation activated Src tyrosine kinase, mediated by ROS in HeLa cells [20]. There are also many studies reporting that laser irradiation regulated the phosphorylation of critical cellular kinases. For example, low-power laser irradiation increased Akt phosphorylation in A-172 cells [24], MAPK/ERK activity in skeletal muscle [25], and Src tyrosine kinase activity in HeLa cells [20]. Increased tyrosine phosphorylation is closely associated with VSM contraction. Src tyrosine kinase was reported to be a critical regulator of rat arterial vasocontraction [11, 12]. The western blotting results in this study also showed that 445 nm laser irradiation induced phosphorylation of tyrosine residues in proteins, including those with the molecular weight of Src tyrosine kinase (Fig. 1(F), Src band-70 kDa).

4.3 Irradiation with the 445 nm diode laser inhibited VLCCs

Above, we discussed the mechanisms of 445 nm laser-induced vasocontraction. In the presence of the endothelium, the activation of eNOS and concomitant activation of oxidative stress mediated laser-induced vasocontraction. In the absence of the endothelium, the 445 nm laser activated PTKs, and the consequent vasocontraction was evident in the presence of a VLCC inhibitor. In the absence of the endothelium, however, the primary response to the 445 nm laser was vasorelaxation (Figs. 1(B) and 4(A)).

The contractile response was only evident after pretreating with a VLCC inhibitor (Fig. 4(B)). This suggests that the 445 nm laser primarily relaxed aortic rings by modulating VLCCs of VSM, in the absence of the endothelium. This hypothesis is supported by the results shown in (Fig. 4(D)). The 445 nm laser inhibited VLCC currents in A7r5 cells. It is still unclear how the 445 nm laser inhibited VLCC currents. One possibility is that laser-induced ROS inhibited VLCC currents. In a preliminary study, we have observed that hydrogen peroxide (H_2O_2) inhibited VLCC currents in A7r5 cells in a concentration-

#242957 Received 18 Jun 2015; revised 12 Aug 2015; accepted 14 Aug 2015; published 21 Aug 2015

dependent manner (unpublished observation), supporting this hypothesis. Further studies on the mechanisms by which laser irradiation regulates VLCC are needed. There are also many studies reporting on ion channel regulation by laser irradiation. For example, 405 nm and green lasers activated TRPV channels and increased the intracellular Ca^{2+} concentration in mast cells [26–28]. TRPV1 is known to open at temperatures over 42°C. However, Gu et al. [26] suggest a direct activation of TRPV1 by the green laser independent of an associated temperature increase, since the temperature increased by at most 0.5°C in this case. In the present study, we used a 445 nm laser with a power output of 300 mW and a spot size of 4 mm. Under these conditions, the temperature increase during the 5 min irradiation period was at most 3°C, which also suggests that a laser-induced temperature increase was not involved in the effects of the 445 nm laser on vascular tone. Further studies are warranted for an accurate understanding of how the energy of the 445 nm laser is converted into biological signals such as eNOS activation, PTK activation, and VLCC inhibition.

5. Conclusions

The 445 nm blue laser exerted multiple effects on aorta blood vessels, resulting in both vasocontraction and vasodilation. Since the different vascular responses to the 445 nm laser were mediated by distinct mechanisms in the endothelium and VSM, the results of the present study might provide useful information for potentially selective and beneficial biomedical applications of the 445 nm laser in the field of laser therapy for vascular diseases.

Acknowledgments

This research was supported by the Pioneer Research Center Program (2011-0027921) through the National Research Foundation of Korea funded by the Ministry of Science, ICT & Future Planning.

#242957 Received 18 Jun 2015; revised 12 Aug 2015; accepted 14 Aug 2015; published 21 Aug 2015